24th INTERNATIONAL CONGRESS ON SOUND AND VIBRATION
23–27 July 2017, London

ICSV24
23-27JULY 2017
LONDON CALLING

ASYMMETRIC FINITE DIFFERENCES FOR NON-CONSTANT-AMPLITUDE WAVES

E.J. Brambley
University of Warwick, Mathematics Institute & WMG, Coventry, UK
email: E.J.Brambley@warwick.ac.uk

Computational AeroAcoustics (CAA) simulations often use finite difference schemes optimized to require relatively few points per wavelength; such schemes are often referred to as Dispersion Relation Preserving (DRP) schemes. Recently, it was shown that such optimized schemes perform poorly when applied to waves with an increasing or decreasing amplitude. Here, we investigate the performance of asymmetric stencils used at the boundaries of the computational domain, by considering a 1D model wave-propagation problem involving damping, propagation over large distances, and reflection by boundaries. Existing optimized boundary stencils are found to be totally unstable for this model problem. A new DRP scheme with the Summation By Parts (SBP) property is derived and proved to be stable. However, as expected, its behaviour is poor for non-constant-amplitude waves, and existing maximal order SBP schemes are shown to be preferable. Consequences for realistic 3D CAA simulations are also discussed.

Keywords: Finite differences, computational aeroacoustics, DRP

1. Introduction

Computational AeroAcoustics (CAA) form an important tool in the design of quiet aircraft engines. Owing to the complicated geometry and flow in aircraft engines, these simulations are computationally demanding, and so it is desired to use as low a numerical resolution as possible to accurately resolve the behaviour of the waves. In the interior of a domain, considering an equi-spaced grid of points $x_j = j\Delta x$ and function evaluations $f_j = f(x_j)$, a symmetric finite difference scheme of width w with coefficients d_m and β_m numerically approximates the derivative $f'(x_j)$ by

$$f'_j + \sum_{m=1}^{B} \beta_m \big(f'_{j+m} + f'_{j-m}\big) = \frac{1}{\Delta x} \sum_{m=1}^{(w-1)/2} d_m \big(f_{j+m} - f_{j-m}\big). \tag{1}$$

Schemes with $B = 1$ are termed tri-diagonal, and schemes with $B = 0$ are termed explicit. Explicit schemes are numerically simpler to calculate, although require more points per wavelength to accurately resolve waves. The finite difference coefficients d_m and β_m are chosen such that f'_j is a good approximation to $f'(x_j)$. Classically one would consider the limit $\Delta x \to 0$ and require $f'_j = f'(x_j) + O(\Delta x^{w+2B-1})$, and such schemes are referred to here as Maximal Order (MO) schemes since they give the maximum order of asymptotic accuracy for a given w and B. An alternative for wave propagation problems is to choose the coefficients d_m such that waves are well resolved with few points per wavelength [e.g. 1–5], and such schemes are frequently referred to as Dispersion Relation Preserving (DRP) schemes [2]. Unfortunately, it was recently pointed out that such DRP schemes perform poorly when simulating non-constant-amplitude waves [6].

At the boundaries of a domain we run out of points, and symmetric stencils can no longer be used. However, care is needed when using asymmetric stencils, as doing so often leads to instability. Provided certain conditions are met, the order of accuracy of the boundary derivatives may be one order less than that of the interior derivatives without affecting the global accuracy of the scheme [7]. As an example, considering the explicit 7-point 6th order symmetric stencil given by $B = 0$ and $(d_1, d_2, d_3) = (\frac{3}{4}, \frac{-3}{20}, \frac{1}{60})$, we require a different formula to calculate f'_0, f'_1, and f'_2. Using 5th order asymmetric stencils to give a global 6th order scheme would result in the derivative

$$\begin{pmatrix} f'_0 \\ f'_1 \\ f'_2 \\ f'_3 \\ f'_4 \\ \vdots \end{pmatrix} = \frac{1}{\Delta x} \begin{pmatrix} -137/60 & 5 & -5 & 10/3 & -5/4 & 1/5 & & \\ -1/5 & -13/12 & 2 & -1 & 1/3 & -1/20 & & \\ 1/20 & -1/2 & -1/3 & 1 & -1/4 & 1/30 & & \\ -1/60 & 3/20 & -3/4 & 0 & 3/4 & -3/20 & 1/60 & \\ & \ddots & \ddots & \ddots & \ddots & \ddots & \ddots & \ddots \end{pmatrix} \begin{pmatrix} f_0 \\ f_1 \\ f_2 \\ f_3 \\ f_4 \\ \vdots \end{pmatrix}. \tag{2}$$

This scheme is referred to as "mo7" in what follows, and it will be seen to be completely unstable. A common alternative is to use symmetric stencils of decreasing width near the boundary, with only f'_0 being calculated using an asymmetric stencil. For the example above, this might be given by

$$\begin{pmatrix} f'_0 \\ f'_1 \\ f'_2 \\ f'_3 \\ f'_4 \\ \vdots \end{pmatrix} = \frac{1}{\Delta x} \begin{pmatrix} -3/2 & 2 & -1/2 & & & & & \\ -1/2 & 0 & 1/2 & & & & & \\ 1/12 & -2/3 & 0 & 2/3 & -1/12 & & & \\ -1/60 & 3/20 & -3/4 & 0 & 3/4 & -3/20 & 1/60 & \\ & \ddots & \ddots & \ddots & \ddots & \ddots & \ddots & \ddots \end{pmatrix} \begin{pmatrix} f_0 \\ f_1 \\ f_2 \\ f_3 \\ f_4 \\ \vdots \end{pmatrix}. \tag{3}$$

This scheme is referred to as "mo7s" in what follows, and it will be seen to be stable, but of rather low accuracy, and asymptotically only of global accuracy $O(\Delta x^3)$.

Asymmetric optimized (DRP) stencils for use at boundaries have been investigated by Berland, Bogey, Marsden & Bailly [8] for explicit schemes, and by Turner, Haeri & Kim [9] for implicit schemes. Here, we consider the 7-point 4th order DRP scheme of Tam & Shen [10] with the 7-point 4th order optimized boundary derivatives of Ref. 8, labelled as "DRP7+BBMB", which we will find to be totally unstable. We also consider the 11-point 4th order FDo11p scheme of Bogey & Bailly [4] with the 11-point 4th order optimized boundary derivatives of Ref. 8, labelled as "BB11+BBMB", which we will also find to be totally unstable. Finally, we consider the 7-point tri-diagonal 4th order optimized scheme of Kim [5] with the 4th order optimized boundary derivatives of Ref. 9, labelled as "K+THK3,7", which we will also find to be totally unstable, both in its basic and pseudo-boundary forms [9, Section 6]. A summary of these schemes is given in Table 1.

As asymmetric stencils are necessary at boundaries, but in general lead to instability, we also consider a recent class of schemes which are provably stable. A brief overview of these Summation By Parts (SBP) schemes is given in Section 2, before we select three such schemes to compare with those above solving a test problem. The test problem, involving wave propagation, damping, and reflection from boundaries, is described in Section 3, with the results presented in Section 4.

2. Summation by Parts

For full details, see the excellent review articles by Svärd & Nordström [11] and Del Rey Fernández, Hicken & Zingg [12]. Here, we consider the domain $[0, L]$ discretized by $N + 1$ equally-spaced points $x_0, \ldots, x_N$. In the interior of the domain a symmetric derivative is used. A different derivative is used for the n points near the boundary, $x_0, \ldots, x_{n-1}$ and $x_{N-n+1}, \ldots, x_N$. In vector form, writing $\boldsymbol{f} = (f_0, \ldots, f_N)$ and $\boldsymbol{f}' = (f'_0, \ldots, f'_N)$, the derivatives are given implicitly by $\Delta x \mathsf{P} \boldsymbol{f}' = \mathsf{Q} \boldsymbol{f}$, so

Table 1: Summary of finite difference schemes considered

Scheme	Reference	w	acc	n	accuracy	SBP	Type
mo7	Equation (2)	7	6	3	5		Expl
mo7s	Equation (3)	7	6	3	2,2,4		Expl
BB11+BBMB	[4, FDo11p] &[8, Table 10]	11	4	5	4		Expl
DRP7+BBMB	[10] & [8, Table 9]	7	4	3	4		Expl
DRP7sbp	Appendix A	7	4	4	3	y	Expl
CGA7sbp	[13, appendix 2]	7	6	6	5	y	Expl
FHZ7sbp	[12, $D_1^{(6,3,:)}$, appendix A]	7	6	6	3	y	Expl
K+THK3,7	[5, Table 1] & [9, Table 2]	7	4	3	4		Tri
K+THKp3,7	[5, Table 1] & [9, Section 6]	7	4	6	4		Tri

Key: w = width of interior stencil; acc = order of accuracy of interior stencil; n = number of points near boundaries not using the interior stencil; accuracy = order of accuracy within n points of the domain boundary; Expl = explicit in the domain interior; Tri = tri-diagonal in the domain interior.

that the differentiation matrix is $\mathsf{D} = \mathsf{P}^{-1}\mathsf{Q}/\Delta x$. The finite difference scheme P, Q is said to have the summation by parts (SBP) property if

$$\mathsf{P} = \text{symmetric, positive definite} \qquad \text{and} \qquad \mathsf{Q} + \mathsf{Q}^T = \boldsymbol{e_N} \boldsymbol{e_N}^T - \boldsymbol{e_0} \boldsymbol{e_0}^T, \tag{4}$$

where $\boldsymbol{e_0} = (1, 0, \ldots, 0)$ and $\boldsymbol{e_N} = (0, \ldots, 0, 1)$; i.e. Q is anti-symmetric except for its $(0,0)$ and (N,N) elements. The SBP scheme is explicit if P is the identity apart from its first and last n rows.

We define the discrete inner product $\langle \boldsymbol{u}, \boldsymbol{v} \rangle_\mathsf{P} = \boldsymbol{u}^T \mathsf{P} \boldsymbol{v} \Delta x$. This is the discrete equivalent of $\langle u, v \rangle = \int_0^L u(x) v(x) \, \mathrm{d}x$, and using Eq. (4) we deduce the discrete analogue to integration by parts,

$$\langle \boldsymbol{u}, \mathsf{D}\boldsymbol{v} \rangle_\mathsf{P} = u_N v_N - u_0 v_0 - \langle \mathsf{D}\boldsymbol{u}, \boldsymbol{v} \rangle_\mathsf{P}, \qquad \text{implying} \qquad \langle \mathbf{1}, \mathsf{D}\boldsymbol{u} \rangle_\mathsf{P} = u_N - u_0 \tag{5}$$

where $\mathbf{1} = (1, 1, \ldots, 1)^T$. The theory then proves long-time stability in the sense that $\langle \boldsymbol{f}, \boldsymbol{f} \rangle_\mathsf{P}$ remains bounded for all time, although this is proved on a case-by-case basis, as we do here in Section 3.1.

It is emphasized that having the SBP property is a strong requirement, and that most boundary schemes are not SBP (including those of Refs. 8 and 9). The SBP stability properties also only hold provided the boundary conditions are implemented appropriately, as discussed in Section 3.

We consider three SBP schemes here. The first is a new SBP scheme given in appendix A which uses the 7-point 4th order DRP stencil of Tam & Shen [10] as the interior stencil, and is denoted "DRP7sbp". The second, denoted "CGA7sbp", is a 7-point 6th order internal scheme which is 5th order within 6 points of the boundary, given by Carpenter, Gottlieb & Abarbanel [13, appendix 2]. The third, denoted "FHZ7sbp", is an SBP scheme with P diagonal that uses the same 7-point 6th order internal scheme but is only 3rd order within 6 points of the boundary, and is given by Del Rey Fernández, Hicken & Zingg [12, $D_1^{(6,3,:)}$, appendix A]. A summary of all schemes used is given in Table 1.

3. Problem description

The example we consider here is that of Ref. 6, only with reflecting boundaries instead of periodic boundaries. We consider on the domain $x \in [0, L]$, $t \geq 0$ the coupled PDEs

$$\frac{\partial p}{\partial t} + \frac{\partial v}{\partial x} = -\mu(x) p, \qquad \frac{\partial v}{\partial t} + \frac{\partial p}{\partial x} = -\nu(x) v, \tag{6}$$

with boundary conditions $v(0,t) = v(L,t) = 0$ and initial conditions $p(x,0) = p^0(x)$ and $v(x,0) = v^0(x)$. For the case $\mu(x) = \nu(x)$ these may be solved analytically; in that case, at time $T = 2L$

it can be shown that $p(x,T) = \mathrm{e}^{-2a}p^0(x)$ and $v(x,T) = \mathrm{e}^{-2a}v^0(x)$, where $a = \int_0^L \mu(x)\,\mathrm{d}x$ is the cumulative damping seen by a wave traversing the domain.

We discretize Eq. (6) in space by dividing $[0, L]$ into $(N+1)$ equally spaced points, $x_j = j\Delta x$. Introducing the derivative operator D given by $\Delta x\mathsf{PD} = \mathsf{Q}$ gives the discretized equations

$$\Delta x\mathsf{P}\frac{\partial \boldsymbol{p}}{\partial t} + \mathsf{Q}\boldsymbol{v} = -\Delta x\mathsf{PM}\boldsymbol{p}, \qquad \Delta x\mathsf{P}\frac{\partial \boldsymbol{v}}{\partial t} + \mathsf{Q}\boldsymbol{p} = -\Delta x\mathsf{PN}\boldsymbol{v}, \tag{7}$$

where M and N are diagonal matrices with diagonals $\mu(x_j)$ and $\nu(x_j)$ respectively.

One way to apply the boundary conditions $v(0,t) = v(L,t) = 0$ is by directly setting $v_0 = v_N = 0$. However, this may break the SBP property that we use below to ensure long-time stability. As an alternative, we enforce the boundary conditions in a weak sense by forcing the right hand side of the Eq. (7) with Simultaneous Approximation Terms (SATs [13]), derived by considering the incoming and outgoing characteristics at the domain edges [12]. This leads to

$$\Delta x\mathsf{P}\frac{\partial \boldsymbol{p}}{\partial t} + \mathsf{Q}\boldsymbol{v} = -\Delta x\mathsf{PM}\boldsymbol{p} - \sigma_0 v_0 \boldsymbol{e_0} + \sigma_L v_N \boldsymbol{e_N}, \tag{8a}$$

$$\Delta x\mathsf{P}\frac{\partial \boldsymbol{v}}{\partial t} + \mathsf{Q}\boldsymbol{p} = -\Delta x\mathsf{PN}\boldsymbol{v} - \sigma_0 v_0 \boldsymbol{e_0} - \sigma_L v_N \boldsymbol{e_N}, \tag{8b}$$

where σ_0 and σ_L dictate the strength of the forcing and are determined below.

3.1 Proof of stability of the SBP/SAT discretized problem

By using integration by parts on Eq. (6) we find a "conserved" energy,

$$\frac{\mathrm{d}}{\mathrm{d}t}\int_0^L \tfrac{1}{2}p^2 + \tfrac{1}{2}v^2\,\mathrm{d}x = -\int_0^L \mu p^2\,\mathrm{d}x - \int_0^L \nu v^2\,\mathrm{d}x. \tag{9}$$

For an SBP operator, by applying the inner product $\langle \boldsymbol{u}, \boldsymbol{v}\rangle_{\mathsf{P}}$ to Eq. (8) and using the SBP property (Eq. 5) we may derive the discrete analogue of Eq. (9),

$$\begin{aligned}\frac{\mathrm{d}}{\mathrm{d}t}\big(\tfrac{1}{2}\langle \boldsymbol{p},\boldsymbol{p}\rangle_{\mathsf{P}} + \tfrac{1}{2}\langle \boldsymbol{v},\boldsymbol{v}\rangle_{\mathsf{P}}\big)& \\ = -\langle \boldsymbol{p}, \mathsf{M}\boldsymbol{p}\rangle_{\mathsf{P}} - \langle \boldsymbol{v}, \mathsf{N}\boldsymbol{v}\rangle_{\mathsf{P}} - (1-\sigma_L)p_N v_N + (1-\sigma_0)p_0 v_0 - \sigma_0 v_0^2 - \sigma_L v_N^2.&\end{aligned} \tag{10}$$

For guaranteed long-time stability we require the right hand side of Eq. (10) to be always non-positive, and therefore we have no choice but to take the SAT strengths to be $\sigma_0 = \sigma_L = 1$.

3.2 Filtering

It is common in CAA simulations to use low-pass filters to remove spurious under-resolved waves from the solution that can lead to instability. While the SBP derivatives give provable stability, as shown above, for a fair comparison all results here use filtering, with the filtering strength tuned to give the best numerical accuracy. The two filters used here are described in detail in Ref. 6. A wide 19-point 16th order symmetric filter labelled s164 is used as a "perfect" filter with errors far smaller than those of the derivative. A standard 7-point 6th order symmetric filter labelled s7 is also used as an example of a filter used in practice. These are applied every timestep with a strength $S\Delta t$, so that the unfiltered solution $\boldsymbol{f}$ becomes the filtered solution $(1 - S\Delta t)\boldsymbol{f} + S\Delta t\mathsf{F}\boldsymbol{f}$, where F is the filter.

Since these filters are symmetric, they cannot be applied at the boundaries of the domain. Rather than complicating matters by using asymmetric or optimized filtering [e.g. 14], no filtering was performed close to the boundaries. This should still give sufficient filtering, as waves move with velocity 1 and therefore spend very few timesteps close to the boundary in the unfiltered region.

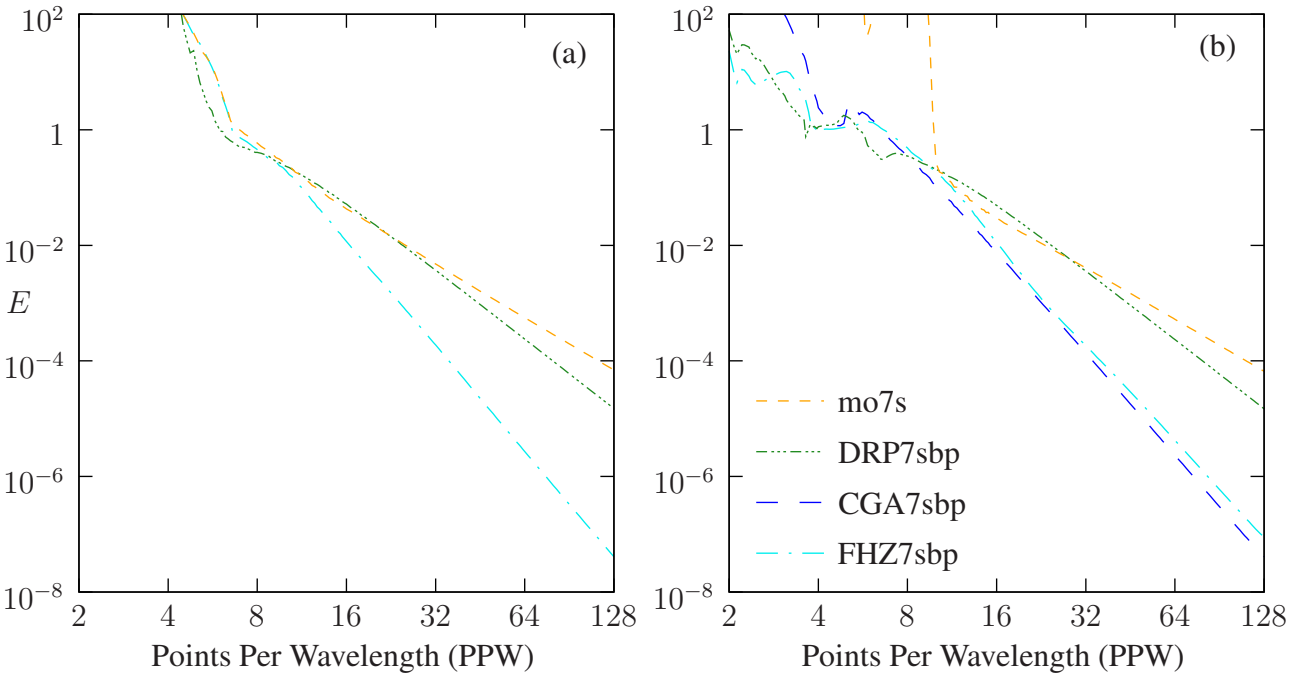

Figure 1: Plot of error (defined in Eq. (11)) against points per wavelength for the "perfect" filter s164 and time integration RK45. (a) applies the boundary conditions directly, while (b) applies the boundary conditions weakly using SATs. The derivative schemes are listed in Table 1. Only schemes which are stable are plotted.

3.3 Parameters and Error Quantification

We use the same parameters as in Ref. 6: the domain length is $L = 24$, and the damping $\mu(x) = \nu(x)$ is smooth and such that $\mu(x) \neq 0$ only for $x \in (20\frac{1}{2}, 23\frac{1}{2})$ with $\int_0^L \mu(x)\,\mathrm{d}x = 6$. Initial conditions are $p^0(x) = v^0(x)$ with a wave packet of wavelength 1 with amplitude smoothly varying and nonzero initially only for $x \in (0, 20)$. As described in Ref. 6, these parameters are chosen to be indicative of decay rates and propagation distances typically found in CAA simulations. Since $\mu(x) = \nu(x)$, at time $T = 48$ the wavepacket should have reflected from both ends of the domain, and comparing with the analytic solution gives an L_∞ error measure

$$E = \sup_{x\in[0,L]} \left\{ \left|p(x,T)\mathrm{e}^{12} - p^0(x)\right|, \left|v(x,T)\mathrm{e}^{12} - v^0(x)\right| \right\}. \tag{11}$$

4. Results

To isolate errors due to the spatial derivative, we first use a "perfect" time integrator and a "perfect" spatial filter. The spatial filter used is the 19-point s164 filter referred to in Section 3.2 above, while an adaptive timestep Runge–Kutta (RK45) with a required accuracy of 10^{-8} was used for the time integration. Figure 1(a) plots the error E from Eq. (11) against the number of points per wavelength N/L when applying the boundary conditions directly. Results were calculated for all derivatives listed in Table 1, with only the three plotted converging. The only non-SBP derivative that converged is the mo7s scheme, which uses lower-order symmetric stencils near the boundaries, although it gives the worst convergence rate of only $O(\Delta x^3)$, as expected. The diagonal SBP derivative FHZ7sbp gives the best performance with an $O(\Delta x^6)$ convergence rate, which is better than the theoretical $O(\Delta x^4)$ rate expected, possibly due to errors being dominated by the interior of the domain in this case. The CGA7sbp SBP operator failed to converge due to the use of directly applied boundary conditions.

Figure 1(b) shows the results when the boundary conditions are applied in the weak SAT sense. All SBP derivatives converged for this case, as expected from the stability proof in Section 3.1. Again the mo7s is the only non-SBP derivative to converge, with a poor $O(\Delta x^3)$ convergence rate. The DRP7sbp scheme converge at its expected $O(\Delta x^4)$ rate, while the FHZ7sbp and CGA7sbp schemes

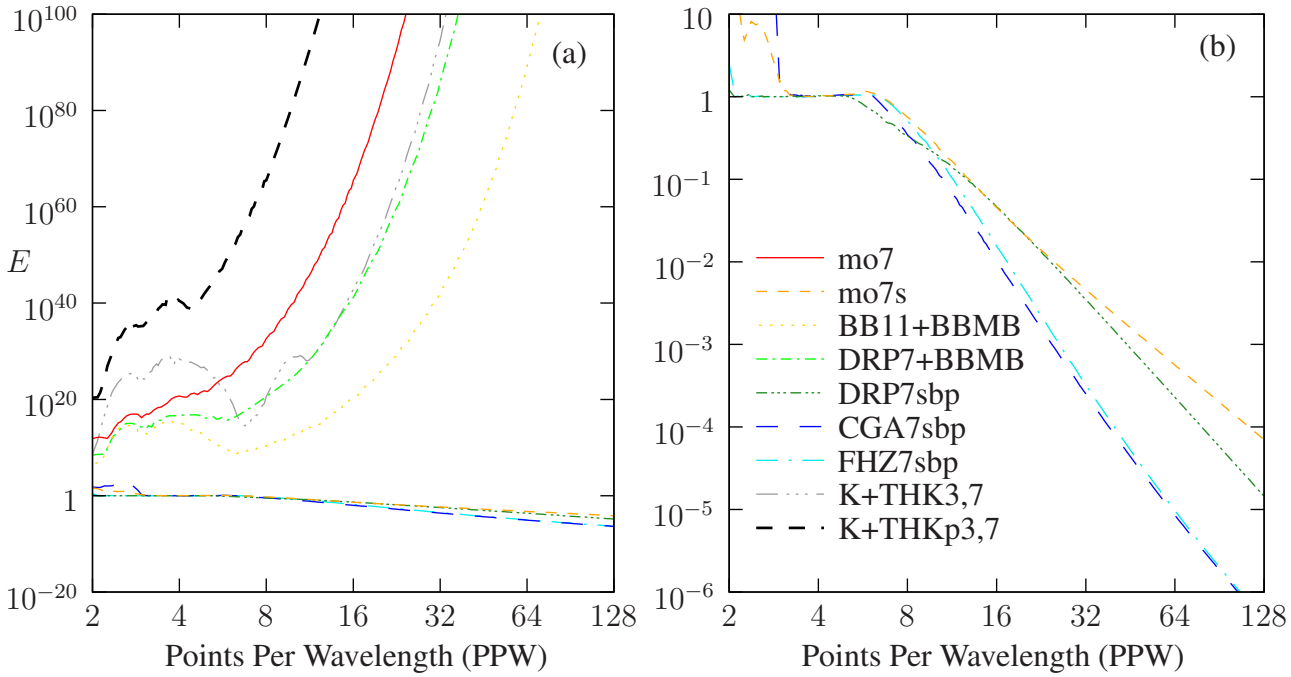

Figure 2: Error (Eq. 11) against PPW for the "real-world" filter s7 and time integration LDDRK56 at CFL $= 0.8$. (a) and (b) plot the same data on different scales. SAT boundary conditions are used for the SBP schemes, direct boundary conditions are used for the others. The derivative schemes are listed in Table 1.

both converge at the rate $O(\Delta x^6)$. There appears to be no disadvantage to imposing the boundary conditions in a weak SAT sense, while this has the advantage over the direct application of boundary conditions that it ensures long-time stability (see Section 3.1).

From Fig. 1 it is clear that, while the SBP DRP scheme is stable, there is no advantage to using an optimized DRP scheme above a maximal order one such as CGA7sbp or FHZ7sbp, as was found for the period case [6]. Indeed, all schemes plotted so far have the same computational cost.

We now consider a real-world case using the standard 7-point 6th order filter s7 (described in Section 3.2) and the fixed-timestep LDDRK56 time integration [15] with a CFL of 0.8. Boundary conditions are imposed using SATs for SBP derivatives, and directly for non-SBP derivatives. Figure 2 plots the error against points per wavelength in this case. Figure 2(a) shows that the non-SBP schemes fail to converge, with the exception of the mo7s scheme mentioned above. This is unfortunate, particularly considering that the DRP7+BBMB and BB11+BBMB schemes use asymmetric stencils at the boundaries particularly designed for wave propagation problems [8] and that the K+THK3,7 and K+THKp3,7 schemes use asymmetric stencils at the boundaries designed with stability in mind [9]. The mo7s scheme again converges with a slow rate $O(\Delta x^3)$, and the DRP7sbp scheme again converges at its theoretical rate of $O(\Delta x^4)$. Both the CGA7sbp and FHZ7sbp schemes initially converge at $O(\Delta x^6)$, before eventually converging at $O(\Delta x^4)$ as the LDDRK56 accuracy becomes the limiting factor. Nevertheless, there is a clear accuracy advantage to using the CGA7sbp and FHZ7sbp schemes. There is again no advantage to using an optimized DRP scheme over a maximal order one.

5. Conclusion

The performance of several finite difference schemes has been compared using a problem involving wave propagation over many wavelengths, exponential damping over a few wavelengths, and wave reflection by boundary conditions. Many finite difference schemes proved unstable due to their choice of asymmetric stencils at the boundaries; this is disappointing, since several had been specifically designed for use at domain boundaries [e.g. 8, 9]. In contrast, a class of finite difference schemes with the Summation By Parts (SBP) property are provably stable and were found to perform well.

Summation By Parts (SBP) schemes have received considerable attention [see, e.g., 11, 12]. In

addition to provable stability they have other beneficial properties, such as the superconvergence of functionals, and their behaviour at the boundaries between two numerical grids. Because of their provable stability, no filtering was needed to stabilize them, although here some filtering was found to enhance their performance. While a number of SBP schemes were found to converge when the boundary conditions were imposed directly on v_0 and v_N, this is not guaranteed in general, and instead other techniques that preserve the SBP property should be used, such as Simultaneous Approximation Terms (SATs). Use of these was necessary for the stability of one SBP scheme, and was not of any significant detriment to any. Note that the strength of the SATs must be exactly specified for the test case used here, as either too weak or too strong would break the provably stable behaviour.

As part of this study, a new SBP scheme was created whose internal symmetric stencil is that of the 7-point 4th order DRP scheme of Tam & Shen [10]. This boundary closure scheme, given in appendix A, may be used for any 7-point 4th order internal scheme by altering the coefficient d_1. Being an SBP scheme it is provably stable, unlike the DRP optimized boundary closure proposed by Berland, Bogey, Marsden & Bailly [8] which was always unstable for the test case used here. However, DRP schemes are known to perform poorly with non-constant-amplitude oscillations [6], and this was confirmed here by the poor performance of the DRP7sbp scheme in Figs 1–2.

Diagonal SBP schemes (where P is diagonal) are important when mapping curvilinear physical coordinates onto a rectangular equi-spaced computational grid [16]. The only diagonal SBP scheme considered here is the FHZ7sbp scheme of Del Rey Fernández, Hicken & Zingg [12, $D_1^{(6,3,:)}$, appendix A]. This scheme uses a 7-point 6th order stencil in the interior, but is only 3rd order accurate for the 6 points closest to the boundary. Nevertheless, in practice it attained 6th order accuracy on the test case used here. This might be due to to the major source of error being within the domain interior for this case, and could not be expected in general. The CGA7sbp scheme uses the same interior stencil but retains theoretical 6th order accuracy overall, although it is not a diagonal scheme.

Realistic 3D CAA simulations contain a wide range of wavelengths and decay rates, especially near boundaries. Since SBP schemes perform so well here, and add little if any complication to the numerical implementation, their use is recommended. It is unlikely that optimized asymmetric boundary stencils [e.g. 8, 9] would show any significant advantage over SBP schemes, since wave amplitudes at boundaries are often non-constant, and even then any advantage in resolution would be outweighed by the major disadvantage of their inherent instability. Despite only using a 4th order time integration, the 6th order finite difference schemes CGA7sbp and FHZ7sbp significantly outperformed their 4th order counterparts (see Fig. 2), particularly for relatively few points per wavelength, and so their use is recommended. The FHZ7sbp scheme has the advantage of being diagonal, while the CGA7sbp scheme has the advantage of being provably globally 6th order accurate. Even in these best cases, at least 16 points per wavelength were needed for an answer accurate to 1%.

A. An SBP closure for 7-point DRP schemes

We find an SBP scheme whose internal stencil is the 7-point 4th order DRP scheme of Tam & Shen [10]. In order to retain global 4th order accuracy we require at least 3rd order accuracy near the boundary. We take a linear combinator of two SBP schemes. The first is a 4th order scheme with 3rd order accuracy near the boundary given by Del Rey Fernández, Hicken & Zingg [12],

$$\mathsf{P}_4 = \begin{pmatrix} \frac{173}{648} & \frac{41}{1296} & 0 & 0 & & & \\ \frac{41}{1296} & \frac{1135}{648} & \frac{-353}{648} & \frac{17}{108} & & & \\ 0 & \frac{-353}{648} & \frac{901}{648} & \frac{-151}{1296} & & & \\ 0 & \frac{17}{108} & \frac{-151}{1296} & \frac{671}{648} & & & \\ & & & & 1 & & \\ & & & & & \ddots & \end{pmatrix} \quad \mathsf{Q}_4 = \begin{pmatrix} \frac{-1}{2} & \frac{2035}{2592} & \frac{-239}{648} & \frac{217}{2592} & & & \\ \frac{-2035}{2592} & 0 & \frac{829}{864} & \frac{-113}{648} & & & \\ \frac{239}{648} & \frac{-829}{864} & 0 & \frac{1747}{2592} & \frac{-1}{12} & & \\ \frac{-217}{2592} & \frac{113}{648} & \frac{-1747}{2592} & 0 & \frac{2}{3} & \frac{-1}{12} & \\ & & \frac{1}{12} & \frac{-2}{3} & 0 & \frac{2}{3} & \frac{-1}{12} \\ & & \ddots & \ddots & \ddots & \ddots & \ddots \end{pmatrix} \tag{12}$$

We construct a similar SBP scheme which is 3rd order accurate near the boundary and 6th order accurate in the interior, given by

$$\mathsf{P}_6 = \begin{pmatrix} \frac{829}{3240} & \frac{601}{6480} & 0 & 0 & & \\ \frac{601}{6480} & \frac{4631}{3240} & \frac{-1189}{3240} & \frac{49}{540} & & \\ 0 & \frac{-1189}{3240} & \frac{865}{648} & \frac{-115}{1296} & & \\ 0 & \frac{49}{540} & \frac{-115}{1296} & \frac{3319}{3240} & & \\ & & & & 1 & \\ & & & & & \ddots \end{pmatrix} \quad \mathsf{Q}_6 = \begin{pmatrix} \frac{-1}{2} & \frac{9347}{12960} & \frac{-943}{3240} & \frac{181}{2592} & & & & \\ \frac{-9347}{12960} & 0 & \frac{4037}{4320} & \frac{-149}{648} & \frac{1}{60} & & & \\ \frac{943}{3240} & \frac{-4037}{4320} & 0 & \frac{10067}{12960} & \frac{-3}{20} & \frac{1}{60} & & \\ \frac{-181}{2592} & \frac{149}{648} & \frac{-10067}{12960} & 0 & \frac{3}{4} & \frac{-3}{20} & \frac{1}{60} & \\ & \frac{-1}{60} & \frac{3}{20} & \frac{-3}{4} & 0 & \frac{3}{4} & \frac{-3}{20} & \frac{1}{60} \\ & \ddots & \ddots & \ddots & \ddots & \ddots & \ddots & \ddots \end{pmatrix} \tag{13}$$

The SBP closure of the 7-point DRP scheme [10] is obtained by setting

$$\mathsf{P} = (9 - 12d_1)\mathsf{P}_4 + (12d_1 - 8)\mathsf{P}_6 \qquad \mathsf{Q} = (9 - 12d_1)\mathsf{Q}_4 + (12d_1 - 8)\mathsf{Q}_6 \tag{14}$$

where $d_1 = 0.77088238051822552$. This scheme is denoted "DRP7sbp" in Figs 1–2.

REFERENCES

1. Vichnevetsky, R. and De Schutter, F., (1975), A frequency analysis of finite element methods for initial value problems. Vichnevetsky, R. (Ed.), *Advances in Computer Methods for Partial Differential Equations*, AICA.
2. Tam, C. K. W. and Webb, J. C. Dispersion-relation-preserving finite difference schemes for computational acoustics, *J. Comput. Phys.*, **107**, 262–281, (1993).
3. Kim, J. W. and Lee, D. J. Optimized compact finite difference schemes with maximum resolution, *AIAA J.*, **34** (5), 887–893, (1996).
4. Bogey, C. and Bailly, C. A family of low dispersive and low dissipative explicit schemes for flow and noise computations, *J. Comput. Phys.*, **194**, 194–214, (2004).
5. Kim, J. W. Optimised boundary compact finite difference schemes for computational aeroacoustics, *J. Comput. Phys.*, **225**, 995–1019, (2007).
6. Brambley, E. J. Optimized finite-difference (DRP) schemes perform poorly for decaying or growing oscillations, *J. Comput. Phys.*, **324**, 258–274, (2016).
7. Gustafsson, B. The convergence rate for difference approximations to mixed initial boundary value problems, *Math. Comput.*, **29** (130), 396–406, (1975).
8. Berland, J., Bogey, C., Marsden, O. and Bailly, C. High-order, low dispersive and low dissipative explicit schemes for multiple-scale and boundary problems, *J. Comput. Phys.*, **224**, 637–662, (2007).
9. Turner, J. M., Haeri, S. and Kim, J. W. Improving the boundary efficiency of a compact finite difference scheme through optimising its composite template, *Computers & Fluids*, **138**, 9–25, (2016).
10. Tam, C. K. W. and Shen, H. Direct computation of nonlinear acoustic pulses using high-order finite difference schemes, (1993).
11. Svärd, M. and Nordström, J. Review of summation-by-parts schemes for initial-boundary-value problem, *J. Comput. Phys.*, **268**, 17–38, (2014).
12. Del Rey Fernández, D. C., Hicken, J. E. and Zingg, D. W. Review of summation-by-parts operators with simultaneous approximation terms for the numerical solution of partial differential equations, *Computers & Fluids*, **95**, 171–196, (2014).
13. Carpenter, M. H., Gottlieb, D. and Abarbanel, S. Time-stable boundary conditions for finite-difference schemes solving hyperbolic systems: Methodology and application to high-order compact schemes, *J. Comput. Phys.*, **111**, 220–236, (1994).
14. Kim, J. W. High-order compact filters with variable cut-off wavenumber and stable boundary treatment, *Computers & Fluids*, **39**, 1168–1182, (2010).
15. Hu, F. Q., Hussaini, M. Y. and Manthey, J. L. Low-dissipation and low-dispersion Runge–Kutta schemes for computational acoustics, *J. Comput. Phys.*, **124**, 177–191, (1996).
16. Svärd, M. On coordinate transformations for summation-by-parts operators, *J. Sci. Comp.*, **20**, 29–42, (2004).